BIOCHEMISTRY
including biophysical chemistry & molecular biology

Article

pubs.acs.org/biochemistry

Cysteine-Mediated Dynamic Hydrogen-Bonding Network in the Active Site of Pin1

Arghya Barman and Donald Hamelberg*

Department of Chemistry and the Center for Biotechnology and Drug Design, Georgia State University, Atlanta, Georgia 30302-4098, United States

Supporting Information

ABSTRACT: Enzymes catalyze a plethora of chemical reactions that are tightly regulated and intricately coupled in biology. Catalysis of phosphorylation-dependent *cis*−*trans* isomerization of peptidyl-prolyl bonds, which act as conformational switches in regulating many post-phosphorylation processes, is considered to be one of the most critical. Pin1 is a *cis*−*trans* isomerase of peptidyl-prolyl(ω-) bonds of phosphorylated-Ser/Thr-Pro motifs and has been implicated in many diseases. Structural and experimental studies are still unable to resolve the mechanistic role and protonation states of two adjacent histidines (His59 and His157) and a cysteine (Cys113) in the active site of Pin1. Here, we show that the protonation state of Cys113 mediates a dynamic hydrogen-bonding network in the active site of Pin1, involving the two adjacent histidines and several other residues that are highly conserved and necessary for catalysis. We have used detailed free energy calculations and molecular dynamics simulations, complementing previous experiments, to resolve the ambiguities in the orientations of the histidines and protonation states of these key active site residues, details that are critical for fully understanding the mechanism of Pin1 and necessary for developing potent inhibitors. Importantly, Cys113 is shown to alternate between the unprotonated and neutral states, unprotonated in free Pin1 and neutral in substrate-bound Pin1. Our results are consistent with experiments and provide an explanation for the chemical reactivity of free Pin1 that is suggested to be necessary for the regulation of the enzyme.

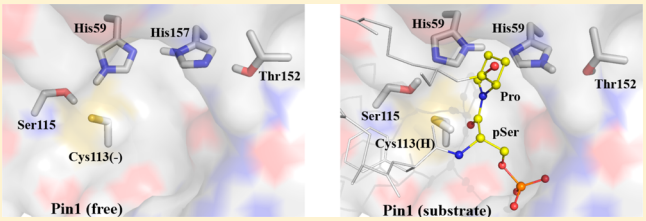

Ionizable residues in proteins, such as Asp, Glu, His, Cys, Lys, Tyr, and Arg, play important chemical roles in a variety of biological processes, including structural stability, solubility, and enzymatic activity.[1] Among these residues, His and Cys in particular have considerable importance because of their unique intrinsic pK_a values of ∼6.5 and ∼8.6, respectively,[2] and because they are typically catalytically active near physiological pH. However, the microenvironment within a protein can alter (upshift or downshift) the pK_a of these residues considerably. Histidine, for example, plays critical roles in enzymecatalysis,[3,4] proton shuttling,[5] proton channel,[6] and hydrogen bonding,[7] and it serves as common ligand in metal coordination.[8,9] In spite of being chemically active, His has additional importance because of it planarity and ability to flip easily (180° rotation around χ2 angle) without changing its spatial occupancy. The imidazole ring of His contains two nitrogen atoms (N_δ and N_ε) and, depending on the pH or the microenvironment, can be neutral and monoprotonated or diprotonated and positively charged. In the neutral form, only one of these two N's can be protonated, whereas both N's are protonated in its cationic form. In addition to the ambiguity of the protonation state of His, the orientation of the imidazole ring is, in most cases, not obvious from X-ray crystallographic structures and is generally assigned to optimize the hydrogen-bonding network. The ambiguities are mainly due to low-resolution X-ray crystal structures and the lack of enough electron density to distinguish between C_δ and N_ε. The rotameric state of His not only has implications for the hydrogen-bonding network but also plays important roles in enzymatic reactions[10−12] and successful virtual screening-based drug design.[13] Similarly, cysteine plays important roles in a number of cellular and subcellular processes, including enzymatic reactions, and its exact protonation state is difficult to assess from experiments. In protein environments, the pK_a of the thiol side chain of cysteine can drop below physiological pH and form an unprotonated, thiolate ion. The unprotonated cysteine can be stabilized by hydrogen bonding, adjacent basic residues, and the surrounding microenvironment in proteins.[14,15] In the thiolate form, Cys becomes more reactive and undergoes reversible (e.g., sulfonation, nitrosylation, and disulfide bond formation) and irreversible (e.g., carbonylation) modifications in several biochemical reactions.[16]

Peptidyl-prolyl *cis*−*trans* isomerases (PPIases) are a family of enzymes that catalyzes the 180° rotation of a peptide bond preceding a proline residue in their protein substrates.[17,18] Pin1 belongs to the parvulin family of PPIases, but it is unique among this class. It binds and catalyzes the *cis*−*trans* isomerization of the peptidyl-prolyl ω-bond when the preceding residue is a phosphorylated Ser (pSer) or phosphorylated Thr (pThr).[18−21] The regulation of phosphorylation-dependent prolyl *cis*−*trans* isomerization by Pin1 is

Received: January 22, 2014
Revised: May 15, 2014
Published: May 19, 2014

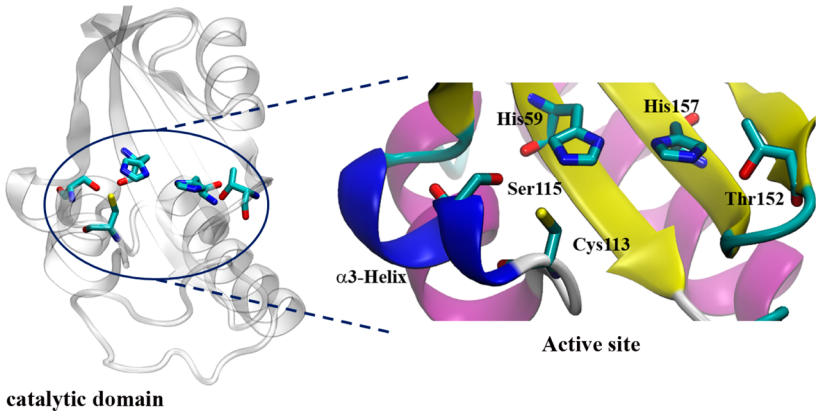

Figure 1. Catalytic domain and active site of Pin1. Residues involved in hydrogen-bonding network in the active site of Pin1 are indicated. Cys113 is located at the N-terminus of the α3-helix (blue).

involved in several cellular signaling pathways, including cell growth and division, DNA repair, apoptosis, and transcription.[22] Pin1 has been directly implicated in many diseases, including cancer[22,23] and Alzheimer's.[24−26] Pin1 is, therefore, a potential therapeutic target for the treatment of many diseases.

Structurally, Pin1 contains two His residues (His59 and His157), lying side by side at the central core of the active site (Figure 1).[27] However, multiple orientations of the His N's are observed in X-ray crystal structures of Pin1 because of ambiguous assignments of the C and N atoms of the imidazole nucleus or because of different crystalline environments. Also, a Cys residue, Cys113, is found within hydrogen-bonding distance of one of the histidines, His59, and located at the N-terminus of α3 helix (Figure 1). These residues are also found to be conserved among all other homologues of Pin1 and are considered to play an important role in catalysis. The mechanism of Pin1 and the role of these highly conserved residues still remain a broad area of research, even after a number of experimental and theoretical studies.[20,28−33]

The histidine residues have been proposed to participate directly in the isomerization process, but mutational studies suggested only a structural role in the active site, despite a large reduction in the catalytic activity after mutation of the two histidines to alanine.[32] On the other hand, Cys113 has been assigned a pivotal role in the mechanism of Pin1.[21] There have been two proposed mechanisms of Pin1, supporting the utilization of Cys113 in covalent and noncovalent catalysis. In the proposed covalent catalysis, Ranganathan et al. suggested an abstraction of the proton from the side chain of Cys113 by a base.[21] The thiolate side chain would then act as a nuclophile and attacks the carbonyl carbon of the peptidyl-prolyl bond of the substrate, resulting in the loss of C−N pseudo-double-bond character.[21] The importance of Cys113 was demonstrated by the mutation of Cys113 to Ala and Ser, resulting in the reduction, not abolition, of catalytic activity relative to wild-type Pin1 by 130- and 20-fold, respectively, raising doubts about the covalent mechanism. Recent kinetic isotope effect studies by Mercedes-Camacho et al. firmly rule out participation of Cys113 as a nucleophile.[33] Additionally, Pin1 remains mainly active after Cys113 was mutated to Asp;[34] therefore, it was suggested that unprotonated Cys113 could destabilize the pseudo-double-bond character of the peptidyl-prolyl bond of the substrate and facilitate isomerization in a noncovalent fashion. Nevertheless, many experiments have suggested the existence of the thiolate form of Cys113 in free Pin1. For example, Pin1 can aggregate because of intermolecular disulfide bond formation,[19] it can form covalent adducts with Juglone (5-hydroxynaphthoquinone),[35] an organic compound, and 4-hydroxynonenal (HNE),[36] a product of lipid oxidation, using Cys113, and it is prone to oxidative modification.[37] All of these observations point to the existence of a reactive Cys113.

In spite of all these studies, the protonation states of His59, His157, and Cys113 in Pin1 and related homologues are unresolved. Mueller et al. estimated the microscopic pK_a of the histidine residues in Pin1 and Par14 (parvulin) and solved a high-resolution crystal structure of the latter.[38] The pK_a's of the histidines suggest a neutral state at physiological pH. Structural superposition of Par14 and Pin1 reveals that Cys113 in Pin1 is Asp74 in Par14 (Figure S1), and the pK_a's of these residues remain unavailable in the literature, to the best of our knowledge. An extended hydrogen-bonding network involving a Asp74···His42···His123···Thr118 motif (Par14 numbering) with a defined directionality was proposed on the basis of the high-resolution X-ray crystal structure of Par14, where the N_ε and N_δ atoms are protonated in His42 and His123, respectively. The unprotonated N_ε atom of His123 is involved in a strong hydrogen bond with Thr118, and the protonated N_ε atom of His42 interacts with Asp74. In Pin1, the protonation behavior of these active site residues, including Cys113, and the directionality of the hydrogen-bonding network remain elusive.

In this study, we have carried out detailed investigation of the protonation states of these key residues in Pin1. In particular, we have addressed (i) the positional ambiguities of the imidazole N atoms of His59 and His157 of Pin1 observed in X-ray crystallographic structures in the Protein Data Bank (PDB) and (ii) the protonation states of His59, His157, and Cys113 and the directionality of the hydrogen-bonding network in the free and substrate-bound forms of Pin1. We have carried out detailed free energy calculations and molecular dynamics (MD) simulations in order to complement experiments, to provide an atomic-level description of the system, and to fully understand the nature of hydrogen bonding network in the active site of Pin1. These studies resolve the ambiguities of the orientations of the imidazole ring of the histidines in the X-ray crystal structures of Pin1 and reveal a dynamic hydrogen-bonding network in the active site that is coupled to the protonation state of Cys113. An active site of Pin1 with fluctuating protonation states of His59, His157, and Cys113 and a dynamic hydrogen-bonding network is presented. These results provide details that are necessary to fully understand the

dx.doi.org/10.1021/bi5000977 | *Biochemistry* 2014, 53, 3839−3850

active site dynamics of Pin1 and to assist in the development of effective inhibitors.

COMPUTATIONAL METHODS

Analysis of Crystal Structures. For the crystal structure analysis, all of the PDB structures of human Pin1 were downloaded from the PDB database. The chains were separated if more than one chain was present in the crystal structure. Including all of the chains and the catalytic domain, a total of 47 crystal structures were considered (see Table S1 for a complete list of PDB files used). Finally, the orientations of the histidine imidazole rings were carefully observed by visual inspection. The initial pK_a of the ionizable residues was estimated using the PROPKA 3.1[39−42] program. PROPKA is a structure-based empirical method for fast prediction of the pK_a of the ionizable residues in a protein. The result of these calculations contains two terms, an unperturbed model pK_a (His = 6.5 and Cys = 9.0) and shift in the pK_a resulting from the perturbed microenvironment.

In addition to PROPKA, more sophisticated prediction software, H++,[43−45] was used to predict the orientation of the histidine residues and the protonation state of the ionizable residues. The H++ server uses multiple steps to predict the protonation states of the ionizable residues based on the pK_a calculation. At the first step, it uses the *reduce*[46] algorithm to flip the O and N atoms of the Asn and Gln residues and N and C atoms of the His residues, which are hard to distinguish from an electron density map, and to optimize the hydrogen-bonding network through van der Waals contacts. The automated server utilizes an implicit solvation model and predicts the pK_a of the ionizable residues in proteins based on self-consistent solution of the Poisson−Boltzmann (PB) equation. Finally, the protonation probabilities are assigned to the individual ionizable residue. In this study, the protonation states of the ionizable His and Cys residues were calculated at physiological pH (pH 7.4) with internal dielectric of $\varepsilon = 4.0$.

Structural Model. The initial model of the Pin1 was taken from a high-resolution (1.5 Å) crystal structure with PDB ID 2Q5A.[27] We considered only the PPIase (catalytic) domain of the enzyme in this study, as NMR and thermodynamic studies showed negligible influence of the WW domain on the catalytic turnover and equilibrium binding constant of the PPIase domain of Pin1.[28,47] The WW domain of the enzyme was, therefore, removed from the crystal structure, and only residues 50−163 were used. A consensus substrate analogue of Pin1, Ac-FFpSPR-Nme, was used in this study. The substrate was modeled from the crystal structure bound peptido-mimetic inhibitor with constrained backbone information.[27] The SPDB viewer[48] program was used to build the substrate. In order to compare our results, we have used a high-resolution (0.8 Å) crystal structure of Par14 (PDB ID: 3UI4).[38]

Free Energy and ΔpK_a Calculations. Calculating the free energy difference between two states represents the favorability of one state over the other. The free energy differences between two protonation states of the histidines (conversion from N_δ-H (HID), N_ε to N_δ, N_ε-H (HIE) and vice versa; partial charges were taken from the HID and HIE form of histidines as defined in the AMBER force field) were calculated using the thermodynamic integration (TI) method with the softcore potential. TI calculates the free energy difference between two states coupled with a nonphysical coordinate λ that corresponds to the transformation of one state to another. The free energy of transformation can be calculated using eq 1

$$\Delta G = \int_0^1 \left\langle \frac{\delta V(\lambda)}{\delta(\lambda)} \right\rangle \mathrm{d}\lambda \tag{1}$$

where angular brackets represent a Boltzmann-weighted average and with the integral typically solved numerically using several simulations at fixed λ values. In this study, we have used nine λ values (0.1, 0.2, ..., 0.9). The λ denotes the coupling parameter, and $V(\lambda)$ denotes the λ-coupling potential function. For each step in the thermodynamic cycle, $\lambda = 0$ with potential function $V(0)$ corresponds to the initial protonation state, and $\lambda = 1$ with potential function $V(1)$ corresponds to the final state of each state. The TI procedure was divided into three steps for each λ: (a) charge removal from the hydrogen atoms from one of the N's of histidine, (b) addition of the hydrogen to the other N of the same histidine, and (c) charge addition on the hydrogen atom. The disappearing and reappearing of the hydrogen atoms were treated with softcore potential (eq 2) that was evoked only during the second step. TI calculations with a sample space of nine different λ values were performed for 1 ns each, and the trapezoid rule was implemented for numerical integration of eq 1.

$$V_{\mathrm{softcore}} = 4\varepsilon(1-\lambda)\left[\frac{1}{\left[\alpha\lambda + \left(\frac{r}{\sigma}\right)^6\right]^2} - \frac{1}{\alpha\lambda + \left(\frac{r}{\sigma}\right)^6}\right] \tag{2}$$

During the pK_a shift calculations, the transformation from the neutral state to charged state of the Cys residue was also performed using the thermodynamic integration method coupled with molecular dynamics simulation,[49,50] where disappearing of the HG atom was treated with softcore potential. The parameter for the thiolate was taken from the CYM-type residue of the cysteine incorporated in AMBER parameter database. The shift in the pK_a values was calculated using the following equation

$$\mathrm{p}K_a\ (\mathrm{Pin1}) - \mathrm{p}K_a\ (\mathrm{model}) = \Delta\Delta G/2.303k_BT$$

where $\Delta\Delta G$ is the relative free energy difference between the changes in free energy in protein matrix and the free model system, k_B is Boltzmann's constant, and T is the temperature. The entire thermodynamic cycle for pK_a shift calculation is shown in Figure S2.

Molecular Dynamics Simulation. All simulations were performed using the AMBER10[51] program with the modified version of the Cornell et al. ff99SB[52] force field. As the dianionic form of the phospho-serine residue is the preferred protonation state of the substrate, optimized force field parameters for the dianionic phosphate group of the phospho-serine residue by Homeyer et al. were considered.[53] The xleap module of the AMBER tool was used to solvate the system in the TIP3P[54] water model in a periodic rectangular box. All of the bonds involving hydrogen were constrained using the SHAKE algorithm.[55] The systems were equilibrated at 300 K, and the Langevin thermostat with a collision frequency of 1 ps^{-1} was used to maintain the temperature.[56] Particle mesh Ewald summation method[57] was used to calculate the electrostatic interactions, and a cut off of 9 Å was used for the nonbonded interactions. All simulations were carried out using the NPT ensemble at a constant pressure of 1 bar, and a time step of 2 fs was used to integrate the equation of motion. These protocols were applied to equilibrate the systems by

dx.doi.org/10.1021/bi5000977 | *Biochemistry* 2014, 53, 3839−3850

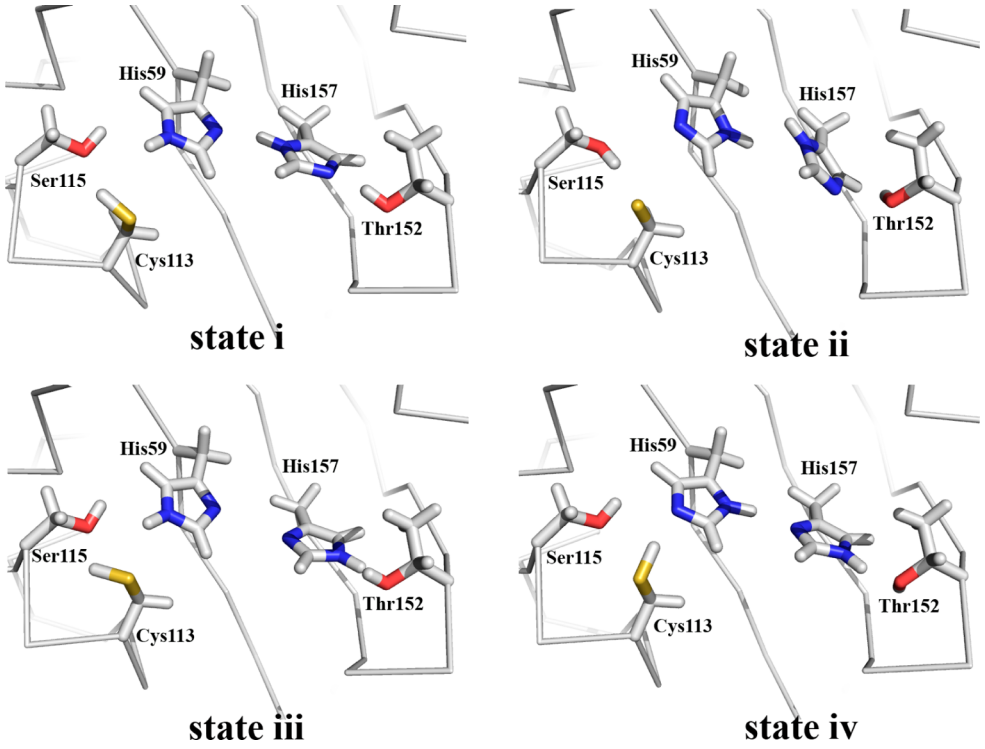

Figure 2. Protonation states of the His residues and Cys113 predicted using the H++ server. The server produced four possible orientations (states i–iv) of the histidine residues and two different protonation states (neutral and unprotonated) of Cys113.

slowly releasing the harmonic constraint of force constant (from 250 to10 kcal/mol/Å^2) applied to the backbone of Pin1 and substrates. Unrestrained simulations were performed for 1 ns before production runs. Finally, the production phases were run for 10 ns, and the last 7 ns of each trajectory was used for analysis. VMD[58] and PyMOL[59] software were used for graphical representations.

RESULTS AND DISCUSSION

Analysis of X-ray Crystal Structures of Pin1. Analysis of 47 crystal structures of Pin1 reveals four possible orientations of the histidines in the active site (states A–D in FigureS3), based on the N's of the imidazole ring of His59 and His157. Consistent discrepancies of the orientations were also observed when we considered only high-resolution X-ray crystal structures (<2.0 Å). Which state is the preferred orientation in solution? The answer to this question is critical because, as a potential drug target, designing inhibitors for Pin1 from structure-based approaches and fully understanding its mechanism of action rely on resolving these ambiguities as well as on an accurate representation of the structural model.

Initially, we used PROPKA 3.1[39−42] to estimate the pK_a of the ionizable residues (His59, His157, and Cys113) in the active site using the static conformations of the crystal structures. The results suggest that both His59 and His157 should be in their neutral states at physiological pH (7.4), albeit a very large range. The predicted pK_a values of Cys113 suggest the possible existence of both neutral (Cys113(H)) and unprotonated Cys113 (Cys113(−)) states at physiological pH. The possibility of Cys113 being unprotonated has been suggested by Rangathan et al., where they proposed that unprotonated Cys113 could act as a nucleophile in the catalytic mechanism of Pin1 through a nucleophilic covalent modification of the substrate.[21] However, this mechanism has been ruled out by recent kinetic isotope effect studies.[33]

In order to make further sense of these results, we used a slightly more sophisticated prediction tool, H++, to optimize the orientations of the histidines during the prediction of the protonation states of the three ionizable residues, also using the static X-ray crystal structures. During the determination of the protonation states, the histidine residues could be reoriented in order to optimize the hydrogen-bonding network. Interestingly, H++ predicted a single orientation of both histidines for all of the crystal structures corresponding to that of state A, where the N_δ atoms on both His59 and His157 were found to face each other (Figure S4). The reproducibility of this orientation was checked using WHATIF's check report[60] and optimal hydrogen-bonding network[61] methods. The results were consistent with those from H++. His59 and His157 were predicted to be in their monoprotonated neutral state in all 47 structures, in good agreement with experimental estimates of the microscopic pK_a values.[38] However, the predicted positions of the hydrogen on either N_δ or N_ε of His59 and His157 by H++ depended on the crystal structure and resulted in ambiguous protonation states for these two residues. Four possible protonation states, namely, states i–iv, were predicted (Figure2). H++ predicts state i (83%) to be the most populated state followed by states iii (9%), iv (6%), and ii (2%) (Table S2). H++ calculations were also carried out on Pin1 in the presence of different inhibitors because the protonation states of the ionizable residues could be perturbed by the chemical nature of the inhibitors.[62] The results suggest that small molecular and peptido-mimetic inhibitors have no significant effect on the protonation of these two histidines compared to the enzyme in the free state. The prediction of the protonation state of Cys113 was inconsistent with respect to

dx.doi.org/10.1021/bi5000977 | *Biochemistry* 2014, 53, 3839−3850

the four possible protonation states of His59 and His157 (Table S2).

Overall, inconsistencies were observed in the protonation states of histidines and Cys113. The variation in the protonation states was also observed in H++ calculations with an internal dielectric of $\varepsilon = 10.0$. The discrepancies in the protonation states are believed to originate from the use of static crystal structures with multiple rotameric states of these ionizable residues, highlighting the danger in relying on a single conformation obtained from a crystal structure for these types of predictions. This issue has also been previously addressed by considering diverse protein conformations, for example, during pK_a calculations.[63] Incorporation of a protein's flexibility in a full-atomistic description of the system in predicting the most plausible protonation state of these residues and verifying the orientations of the histidines are essential. Therefore, to obtain consistent results, more detailed free energy calculations and molecular dynamics simulations in explicit solvent were carried out.

Cysteine Mediates Dynamic Hydrogen-Bonding Network. A thermodynamic cycle connecting all of the possible protonation states of the histidines is shown in Figure 3. The

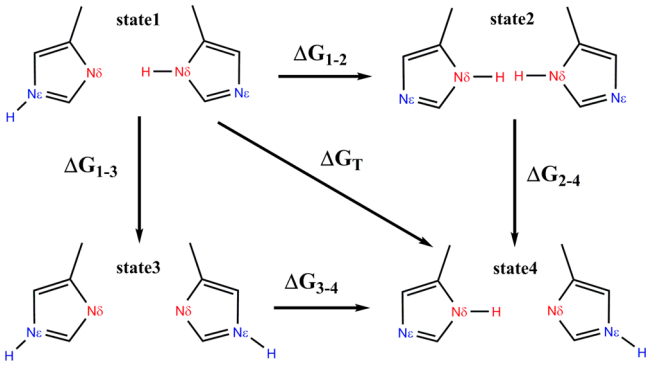

Figure 3. Thermodynamic cycles of inter-state conversion of histidine protonation states.

calculated free energies using TI (see the Computational Methods section) are provided in Table 1. In the free form of Pin1, the free energy of going from state 1 to state 2 is highly unfavorable ($\Delta G_{1-2(\text{free-Cys(H)})} = 5.36 \pm 0.12$ kcal/mol) because of the loss of the hydrogen bond between the histidines and an unfavorable close contact between the N_δ protons of His59 and His157. The free energy change of going from state 1 to state 3 is also associated with the breaking of the hydrogen bond between His59 and His157 ($\Delta G_{1-3(\text{free-Cys(H)})} = 2.08 \pm 0.17$ kcal/mol), which is also unfavorable. As one would expect, the free energy of going from state 3 to state 4 ($\Delta G_{3-4(\text{free-Cys(H)})} = -3.80 \pm 0.16$ kcal/mol) is favorable because of reconstitution of the hydrogen bond between His59 and His157. The resulting free energy from state 2 to state 4, in completing the thermodynamic cycle, is predicted from the other calculated free energies to be $\Delta G_{2-4(\text{free-Cys(H)})} = -7.08 \pm 0.20$ kcal/mol. This change involves a transition from a highly unfavorable state to a state that regains the hydrogen-bonding network and removes the close contacts between the hydrogen atoms on N_δ of the histidines. To verify our predicted results and to get a sense of the errors in the calculations, we also calculated the free energy of going from state 2 to state 4. We obtained a free energy change of $\Delta G_{2-4(\text{free-Cys(H)})} = -6.92 \pm 0.28$ kcal/mol, which is in very good agreement with the predicted free energy. The predicted and calculated free energies are within the limit of the estimated errors and provide a test of the convergence of our calculations.

Any of these pathways can therefore be used to calculate the free energy of going from state 1 to state 4 (ΔG_T). Here, we have used state 2 as the intermediate state. The free energy was calculated to be $\Delta G_{T(\text{free-Cys(H)})} = -1.56 \pm 0.26$ kcal/mol, suggesting that state 4 is more favorable than state 1 in the free form of Pin1,when Cys113(H) is neutral. However, the favorability of state 4 in free Pin1 over state 1 is not in agreement with the previous X-ray crystallographic study of the homologous Par14 by Mueller et al. In that study, Mueller et al. proposed a shared and extended hydrogen-bonding network in the active site of parvulins and Pin1,[38] based on a 0.8 Å X-ray crystal structure of Par14 and pK_a measurements of the histidine residues. The structural study suggested state 1 to be the favored state of the histidines in parvulins. As discussed earlier, parvulins and Pin1 are structurally homologous, with the Cys113 in Pin1 replaced by Asp74 in Par14 (Figure S1). In order to understand the inconsistency between these initial simulation results and experiments, free energy calculations were carried out on Par14. The free energy change from state 1 to state 4 in Par14 was computed, and the result ($\Delta G_{T(\text{par-Asp})} = 1.28 \pm 0.24$ kcal/mol) shows that for Par14, which has an Asp74 (unprotonated) in place of Cys113, the protonation states of the histidines are switched and that state 1 is more favorable than state 4. The result is in complete agreement with the experimental observation by Mueller et al. The incongruity in ΔG_T between Pin1 and Par14 clearly suggests that the protonation states of Cys in Pin1 and Asp in parvulins play an important role in controlling the directionality of the hydrogen-bonding network involving His59 and His157. The effect of the protonation state of Cys113 in Pin1 was investigated by redoing the above free energy calculations using the unprotonated state of Cys113(−). In free Pin1, state 1 now becomes energetically more favorable than state 4 ($\Delta G_{T(\text{free-Cys}(-))} = 4.35 \pm 0.52$ kcal/mol), similar to the result

Table 1. Calculated Free Energies for the Thermodynamic Cycle[a]

		ΔG_{1-2}	ΔG_{2-4}	ΔG_{1-3}	ΔG_{3-4}	ΔG_T
free	Cys(H)	5.36 ± 0.12	−6.92 ± 0.28 (−7.08 ± 0.20)[b]	2.08 ± 0.17	−3.80 ± 0.16	−1.56 ± 0.26
	Cys(−)	7.93 ± 0.38	−3.58 ± 0.88			4.35 ± 0.52
par14	Asp	4.58 ± 0.42	−3.30 ± 0.10			1.28 ± 0.24
sub-*cis*	Cys(H)	7.74 ± 0.10	−10.40 ± 0.37			−2.93 ± 0.48
	Cys(−)	6.07 ± 0.33	−0.13 ± 0.73			5.93 ± 0.99
sub-*trans*	Cys(H)	4.69 ± 0.51	−4.34 ± 0.20			0.35 ± 0.32
	Cys(−)	8.43 ± 0.35	−4.30 ± 0.18			4.13 ± 0.23

[a]Energies are in kilocalories per mole. [b]Predicted free energy from complete thermodynamic cycle.

dx.doi.org/10.1021/bi5000977 | *Biochemistry* 2014, 53, 3839−3850

Table 2. Calculated Free Energies of Each Step in Thermodynamic Cycle for pK_a Calculations[a]

	ΔG_a	ΔG_c	ΔG_t	$\Delta\Delta G$	ΔpK_a
free	−1.56 ± 0.26	−85.92 ± 0.10	−84.36 ± 0.35	−4.13 ± 0.33	−3.01 ± 0.24
sub-*cis*	−2.93 ± 0.48	−83.70 ± 0.65	−80.77 ± 0.84	−0.55 ± 0.96	−0.40 ± 0.70
sub-*trans*	0.35 ± 0.32	−81.03 ± 0.40	−81.38 ± 0.70	−1.16 ± 0.58	−0.84 ± 0.42
sub-*trans*		−81.03 ± 0.40		−0.80 ± 0.28	−0.59 ± 0.20

[a] ΔG_{model} = −80.27 ± 0.05. Energies are in kilocalories per mole. ΔpK_a values were calculated using the formula $\Delta pK_a = \Delta\Delta G/2.303k_BT$, where k_B is Boltzmann's constant and T is the temperature.

obtained for Par14. The favorability of state 1 over state 4, when Cys113(−) is unprotonated, clearly suggests that the protonation state of the residue at this position controls the directionality of the hydrogen-bonding network in the active site of Pin1.

The protonation states of the histidines and the direction of the hydrogen-bonding network were also investigated in the presence of a well-studied substrate analogue with a consensus sequence, Ac-FFpSPR-Nme, in the neutral and unprotonated states of Cys113 in Pin1. In the *cis* configuration of the substrate and with neutral Cys113(H), state 4 was found to be $\Delta G_{T(subcis\text{-}Cys(H))}$ = −2.93 ± 0.48 kcal/mol more favorable than the state 1 (Table 1). On the other hand, state 1 is highly more favored than state 4 ($\Delta G_{T(subcis\text{-}Cys(-))}$ = 5.93 ± 0.99 kcal/mol; Table 1) when Cys113(−) is unprotonated and in the presence of the substrate in the *cis* configuration. States 1 and 4 were almost isoenergetic ($\Delta G_{T(subtrans\text{-}Cys(H))}$ = 0.35 ± 0.32 kcal/mol) in the presence of the substrate in the *trans* configuration whenCys113(H) is neutral. However, state 1 is preferred to state 4 ($\Delta G_{T(subtrans\text{-}Cys(-))}$ = 4.13 ± 0.23 kcal/mol) when Cys113(−) is unprotonated and the *trans* configuration of the substrate is in the active site.

These detailed free energy calculations, which were all carried out in triplicate, clearly show that the orientation of the hydrogen-bonding network in the active site of Pin1 depends on the protonation state of Cys113. State 4 is more favorable than state 1 in both the free and the substrate-bound enzyme when Cys113 is neutral, whereas state 1 is more favorable when Cys113(−) is unprotonated. Although these results clearly show that Cys113 mediates the orientation of the protonation states of the histidine residues, the preferred protonation state of Cys113 in solution (free and substrate-bound) will depend on its microscopic pK_a, which is still not known and difficult to measure experimentally. In order to fully understand the exact nature of the hydrogen-bonding network, insights into the effect of the active site environment of Pin1 on the pK_a of Cys113 are necessary.

pK_a of Cys113 in the Free and Substrate-Bound Forms of Pin1 Differs. Determining the effect of the microenvironment of a protein on the pK_a of ionizable residues is necessary to fully understand its function. We have determined the preferred protonation state of Cys113 in the free and substrate-bound forms of Pin1 as a result of the active site environment in order to fully understand its role, if any, in the active site of Pin1. We calculated the perturbation of the pK_a of Cys113 in the free and substrate-bound forms of Pin1 from free cysteine in solution. The pK_a shifts were calculated on the basis of the free energy of the thermodynamic cycle in FigureS2. The $\Delta\Delta G$, which is related to the change in pK_a (ΔpK_a) by $\Delta pK_a = \Delta\Delta G/(2.303k_BT)$, corresponds to the relative change in the free energy of going from the neutral state to the unprotonated state of Cys113 in a free model amino acid and in the protein.[49,50]

The results of the pK_a calculations are summarized in Table 2. In free Pin1, the pK_a of Cys113 significantly dropped by ∼3 pK_a units relative to that of free cysteine in solution. A negligible drop of ∼0.40 pK_a unit was observed in the presence of the substrate in the *cis* configuration. Similarly, the pK_a dropped ∼0.84 and ∼0.59 pK_a units when the substrate was in the *trans* configuration in states 1 and 4 of the histidines, respectively. The large shift in the pK_a clearly suggests that Cys113(−) prefers to be unprotonated in free Pin1, whereas a less than 1 unit pK_a drop suggests a neutral Cys113(H) in the presence of the substrate.

These results suggest that Cys113 can alternate between thiolate and thiol forms in the active site of Pin1 because of the strong dependence of its pK_a on the active site environment. In the free form of Pin1, Cys113 adopts the unprotonated, thiolate form, which favors the hydrogen-bonding network depicted by state 1. On the other hand, the neutral form of Cys113 is more stable in the Pin1−substrate-bound complex, favoring the state 4 when the substrate is in the *cis* configuration and both states 1 and 4 when the substrate is in the *trans* configuration. This surprising occurrence of the thiolate ion of Cys113 in the free form of Pin1 led us to investigate the microenvironment of the active site in more detail.

Interestingly, the existence of the thiolate form of Cys113 in free Pin1 is consistent with experiments and helps to fully explain experimental observations. Several studies have already suggested that the microenvironment around cysteine residues in the protein could have significant influence on the pK_a of the side chain. A number of factors are known to perturb the pK_a of cysteine residues, including charge−charge interactions, hydrogen bonds, aqueous solvation/desolvation, and the dipole from an α-helix.[14,15] Experimental and structural studies have suggested that cysteines with low pK_a's are normally stabilized by simple hydrogen bonds and electrostatics from the N-terminus of α-helices, along with hydrogen bonds from backbone amides.[64] It is therefore evident that neighboring residues as well as the surrounding environment play important role in determining the protonation equilibria of cysteine residues. Cys113 in Pin1 is located at the N-terminus of the α3 helix and is positioned within hydrogen-bonding distances from Ser115 and His59 (Figure 1). The dipole of α3 helix, hydrogen bonds from Ser115 and His59, and solvents are expected to have significant effect in stabilizing the thiolate ion of Cys113 in free Pin1. The existence of a reactive thiolate ion in Pin1 is supported by the formation of a covalent adduct by the thiol-modifying inhibitor, Juglone,[35] and a lipid electrophile, HNE.[36] Previous study by Bayer et al. also suggested the existence of Cys113 with a low pK_a that participates in local unfolding and formation of an intermolecular disulfide linkage and aggregation.[19] In addition, oxidative modification of Pin1, *in vivo* and *in vitro*, that is suggested to be involved in the regulation of the enzyme also points to the existence of highly reactive species within the enzyme.[37]

dx.doi.org/10.1021/bi5000977 | *Biochemistry* 2014, 53, 3839−3850

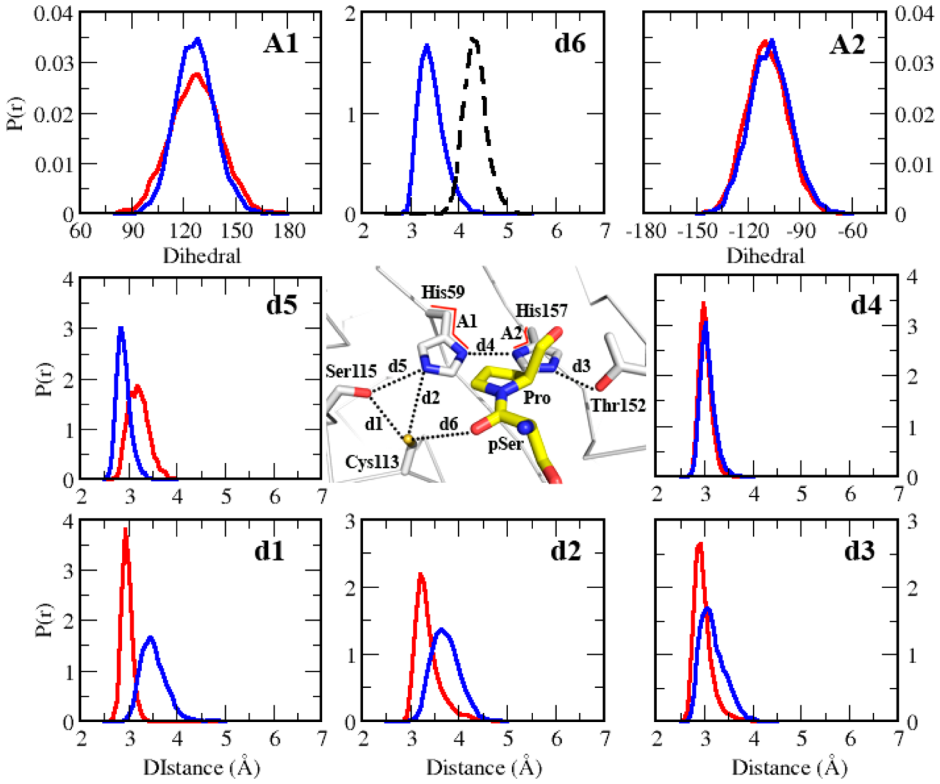

Figure 4. Probability distributions of hydrogen-bond distances (heteroatomic distances) and dihedral angles of His59 and His157. d1 and d2 correspond to the distance between the O of Ser115 and N_ε of His59 and S of Cys113, respectively. d3 represents the distance between N_ε of His157 and O of Thr152. d4 indicates the distance between N_δ of His59 and N_δ of His157. d5 represents the distance between S of Cys113 and N_ε of His59. d6 represents the distance between the S of Cys113 and carbonyl O of the pSer substrate. Probability distributions of dihedral angles of His59 and His157 are shown in A1 and A2. The red color in the graphs signifies free Pin1 (in absence of substrate) with unprotonated Cys113(−), whereas the blue color represents the *cis* configuration bound to Pin1 when Cys113(H) is neutral. The black dotted line in d6 corresponds to the distance in the presence of the substrate in the *cis* configuration when Cys113(−) is unprotonated. The active site residues of Pin1 are shown in white, and the substrate is shown in yellow.

Although the thiolate ion is preferred in the free form of Pin1, the small drop in the pK_a in the presence of the substrate suggests that the microenvironment near Cys113 perturbs the pK_a back to the pK_a of the free amino acid in solution, preferring the neutral form. The source of perturbation may be due to the side chain of pSer upon binding and the subsequent desolvation of the thiolate ion. In the presence of the substrate in the *cis* configuration, the partial electronegative charge on the carbonyl oxygen and highly electronegative phosphate ion influence the local environment of the cysteine thiolate and increase the pK_a of Cys113 to reduce the charge−charge repulsion. Bayer et al. suggested that, in the presence of a sulfate ion in the phosphate binding site of Pin1, the pK_a of Cys113 could be increased, reducing its nucleophilic character.[19] In addition to the charge−charge interaction, the solvent-exposed charged thiolate ion is desolvated upon substrate binding, favoring a higher pK_a of Cys113. The mutual effects of these two factors are seen to be present when the substrate is in the *cis* configuration, in addition to a hydrogen bond between the side chain of Cys113 and the carbonyl oxygen of the peptidyl-prolyl bond. This hydrogen bond is lost when the substrate is in the *trans* configuration, and the loss of the hydrogen bond is slightly observed in the pK_a of Cys113, which is still in the neutral state. The effects of alternative protonation states of the histidines and cysteine on the dynamics of the active site of Pin1 are further explored using all-atom molecular dynamics simulations.

Active Site Integrity in Free and Enzyme−Substrate-Bound Forms of Pin1. In order to understand the integrity of the active site of Pin1 in the different protonation states of Cys113 further, we have carried out MD simulations of free and *cis* substrate-bound Pin1 in states 1 and 4 of the histidines, respectively. The dynamical motions of the active site in free and substrate-bound Pin1 were characterized using hydrogen bonds between key residues in the active site, and the distributions of the corresponding distances are shown in Figure 4.

In the presence of unprotonated Cys113(−) in free Pin1, distances d1, d2, and d3 show narrower distributions, which suggest relatively stronger hydrogen bonds between Cys113 and Ser115 and His59 and between His157 and Thr152, respectively, relative to those in substrate-bound Pin1. In addition to the hydrogen bonds formed between Cys113(−) and Ser115 and His59, three water molecules also are observed to form hydrogen bonds with Cys113(−) in free Pin1 (Figure S5A). These strong hydrogen bonds around Cys113 help to stabilize the thiolate ion, explaining the drop of ∼3 pK_a units in free Pin1. During the time evolution of the hydrogen bonds in free Pin1, the −OH of Thr152 interacts with the N_ε of His157 (d3). This interaction is reversed in the substrate-bound Pin1, where N_ε-H of His157 interacts with the O of Thr152 (Figure S5B). On the other hand, distance d4 and dihedrals A1 and A2 show significant overlap between free and substrate-bound Pin1. These distributions clearly indicate a strong hydrogen

dx.doi.org/10.1021/bi5000977 | *Biochemistry* 2014, 53, 3839−3850

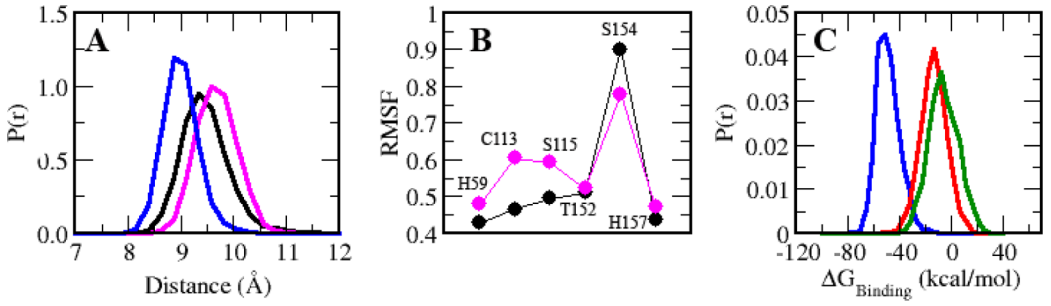

Figure 5. (A) Probability distributions of the Cα distances between Cys113 and Ser154. Black represents free Pin1 with unprotonated Cys113(−), magenta represents free pin1 with neutral Cys113(H), and blue represents *cis* substrate bound by Pin1 with protonated Cys113. (B) Side chain root-mean-squared fluctuation (RMSF) of the active site residues in Pin1. (C) Estimated binding free energies of the *cis* substrate-bound (blue, state 4)) and *trans* substrate-bound (red, state 4; green, state 1) forms.

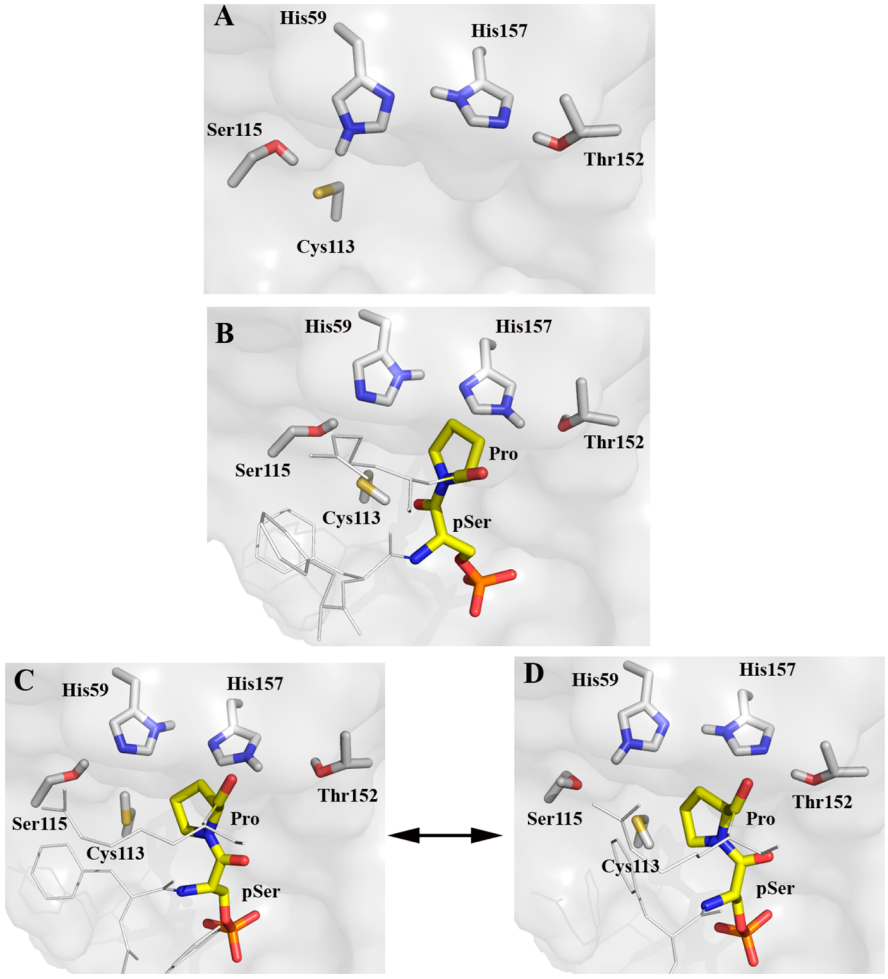

Figure 6. Proposed functional dynamic hydrogen-bonding network in Pin1. (A) In free Pin1, the Cys113 is unprotonated, and the hydrogen-bond network favors state 1. (B) In the presence of *cis* substrate, Cys113 is neutral, and the hydrogen-bond network is in state 4. (C) In the presence of tightly bound *trans* substrate, Cys113 remains neutral, and the hydrogen-bond network is in state 4. (D) Weakly bound *trans* substrate favors the state 1 hydrogen-bond network. Active site residues are shown in white, and the substrate is shown in yellow.

bond between His59 and His157, maintained by the planarity of the imidazole rings. The strength of this hydrogen bond remains the same irrespective of the protonation state of the histidines. Of all the measured distances, d5 is the only distance that shows a narrower distribution in the presence of the substrate in the *cis* configuration, suggesting a stronger interaction between Ser115 and His59 and slightly weaker interactions between Ser115 and Cys113(H) (d1) and between His59 and Cys113(H) (d2). The d6 distance clearly shows that the loss in hydrogen-bonding interactions allows the neutral Cys113(H) to interact with the carbonyl O of pSer of the substrate in the *cis* configuration (Figure S5B).The occupancy of the thiol −SH suggests that the neutral Cys113(H) is oriented toward the carbonyl O of pSer (Figure S6A). On the other hand, the angle between the Cys113 S−H and carbonyl O of pSer below 150° suggests this hydrogen bond is relatively weak (Figure S6B). This weak hydrogen bond between Cys113 and carbonyl O of pSer has also been observed in previous

dx.doi.org/10.1021/bi5000977 | *Biochemistry* 2014, 53, 3839−3850

studies.[30,31] The weak thiol interaction with the carbonyl oxygen of the substrate explains why a Cys113Ser mutation is still active with ~20-fold reduction in the reaction rate.[21] The Cys113Ser mutant suggests a stronger hydrogen bond between the Ser and carbonyl O of the substrate, stabilizing the *cis* configuration. This hydrogen bond is not formed when the substrate is in the *trans* configuration. In addition to the neutral Cys113(H), another simulation was carried out in the presence of the *cis* substrate when Cys113 was unprotonated. When Cys113(−) is unprotonated, d6 is increased because of the repulsion between the negatively charged thiolate and carbonyl O of pSer. Moreover, in the presence of unprotonated Cys113(−) and the *cis* substrate, the distributions of d1, d2, d3, d4, and d5 indicate that the enzyme active site behaves similarly to that of free Pin1 (Figure S7).

In the presence of the substrate in the *cis* configuration, the side chain of Ser154 was observed to interact with the phosphate group of the substrate (Figure S6C). As both Cys113 and Ser154 are in close proximity with the substrate and are located at opposite ends of the active site, the distance between their Cα atoms was chosen to measure the compactness of the active site of Pin1. The distribution of this distance shows that the active site of free Pin1, when Cys113(H) is neutral, is much wider than the that of substrate-bound Pin1, whereas the distance in free Pin1, when Cys113(−) is unprotonated, has a partial overlap between these two states (Figure 5A). This result indicates that the active site of free Pin1 is more compact and closer to that of substrate-bound Pin1. The root-mean-squared fluctuation (RMSF) describes the flexibility of the residues during simulations. The compactness of the active site of free Pin1 when Cys113(−) is unprotonated is also supported by relatively more ordered (lower RMSF) side chains of His59, Cys113, Ser115, Thr152, His157, and Ser154 compared to those of the free Pin1 when Cys113(H) is neutral (Figure 5B).

In addition to the active site integrity, the preference of the substrate in the *trans* configuration for both states 1 and 4 motivated us to look for the most favorable states of the substrate-bound Pin1 based on the binding free energies. We have used the MM/PBSA method[65] to estimate the binding free energies between the substrate in the *cis* and *trans* configurations and Pin1. The distributions of the calculated binding free energies are shown in Figure 5C. The $\Delta G_{binding}$ of the *cis* configuration of the substrate is lower than that of the *trans* configuration, suggesting a discrete preference for the *cis* configuration over the *trans* configuration, which is in excellent agreement with experiments.[28,66,67] The binding free energy distributions of the substrate in the *trans* configuration when the histidines are in states 1 and 4 significantly overlap, with a slight favorability for the *trans* substrate in state 4.

Cysteine-Mediated Dynamic Hydrogen-Bonding Network during Turnover of Pin1 Enzyme. We propose a complete picture of Pin1 enzymatic turnover based on the shifting the pK_a of Cys113 and how it mediates the dynamic hydrogen-bonding network (Figure 6). In the free (or resting) form of the enzyme, Cys113 is unprotonated, and the protonation states of His59 and His157 are in state 1, which is consistent with experimental observations. State 1 corresponds to the protonated N_ε and N_δ atoms of His59 and His157, respectively. In this form, the thiolate of Cys113(−) interacts with Ser115 and His59 through hydrogen bonds. The unprotonated N_δ of His59 acts as hydrogen-bond acceptor from N_δ-H of His157, and the −OH of Thr152 forms a hydrogen bond with the N_ε of His157 to complete the hydrogen-bonding network and stabilized the structural integrity of the active site. Upon binding the substrate in the *cis* configuration, Cys113 becomes neutral, and the protonation states of the histidine residues switch to state 4. In state 4, the hydrogen-bonding network is altered because of changes in the protonation states of the histidines. In state 4, the N_δ atom of His59 is protonated and forms a hydrogen bond with the unprotonated N_δ of His157, whereas the N_ε-H atom of His157 interacts with Thr152. The interaction between Ser115 and Cys113 is lost, and Ser115 forms a hydrogen bond with N_ε of His59. The −SH of neutral Cys113(H), on the other hand, interacts weakly with the carbonyl oxygen of the substrate. In the substrate-bound form, the hydrogen-bonding network becomes relaxed compared to that of the free form of Pin1 to carry out the catalytic turnover from *cis* to *trans*. After the isomerization, the protonation behavior of the histidines can easily adopt either state 1 or state 4 in the presence of the substrate in the *trans* configuration. According to the estimated binding free energies, the substrate in the *trans* configuration is slightly more tightly bound to the enzyme in state 4 than in state 1. Finally, the weaker binding state 1 of the substrate in the *trans* configuration can be released, and the enzyme goes back to its original resting state (Cys113(−)) and state 1 or catalyzes the substrate in the *trans* configuration back to the *cis* configuration.

CONCLUSIONS

We have proposed a cysteine-mediated dynamic hydrogen-bond network in the active site of Pin1. In this study, we have addressed several important and elusive questions of Pin1, ranging from confusing ambiguities about the orientations of two highly conserved active site histidines (His59 and His157) to their protonation states and that of a conserved active site cysteine residue that form a critical hydrogen-bonding network. The overall results obtained from this study reveal a dynamic hydrogen-bonding network in the active site of Pin1 during the functional cycle of Pin1. The dynamic hydrogen-bonding network is mediated by the protonation state of Cys113. The microenvironmental electrostatic effects of the neighboring residues, including the substrate, have significant impact on the perturbation of the pK_a of active site residues. Perturbation of the pK_a of Cys113 indicates an unprotonated Cys113(−) in the free form of Pin1 that is suggested to be involved in the regulation of the enzyme. The pK_a is perturbed to the neutral Cys113(H) form in the presence of the substrate. The results are also in agreement with recent kinetic isotope effect study, because Cys113 was found to be neutral with bound substrate and thus unlikely to act as a nucleophile.[33] On the other hand, the behavior of the protonation states of His59 and His157 is highly dependent on the protonation state of Cys113. Finally, on the basis of the dynamic behavior of these ionizable residues and the estimated binding affinities of the substrate in the different configurations, we propose a complete turnover cycle of Pin1 involving a dynamic hydrogen-bonding network in the active site. The proposed cycle adds a new dimension to the understanding of the functional details of Pin1 as well as to the characterization of this therapeutically important enzyme that will advance efforts in developing new classes of inhibitors.

dx.doi.org/10.1021/bi5000977 | *Biochemistry* 2014, 53, 3839−3850

■ ASSOCIATED CONTENT

Supporting Information

Comparison of Pin1 and Par14 X-ray crystal structure (SI Figure S1) and thermodynamic cycle of pK_a shift calculation (SI Figure S2). Orientations of His59 and His157 in Pin1 (SI Figures S3 and S4). Hydrogen-bond network in free and substrate-bound Pin1 (SI Figures S5 and S6). Distance distribution in the presence of unprotonated Cys113(−) (SI Figure S7). Total number of PDB structure used and results from H++ server calculation (SI Tables 1 and 2). This material is available free of charge via the Internet at http://pubs.acs.org.

■ AUTHOR INFORMATION

Corresponding Author

*E-mail: dhamelberg@gsu.edu; Tel: 404-413-4464; Fax: 404-513-5505.

Funding

This work is supported in part by the National Science Foundation (MCB-0953061) and Georgia Cancer Coalition. This work was also supported by Georgia State's IBM System p7 supercomputer, acquired through a partnership of the Southeastern Universities Research Association and IBM supporting the SURA grid initiative.

Notes

The authors declare no competing financial interest.

■ ACKNOWLEDGMENTS

We thank Dr. Barry Grant for fruitful discussions and suggestions regarding this work.

■ ABBREVIATIONS USED

MD, molecular dynamics; PDB, Protein Data Bank; PME, particle mesh Ewald; pSer, phospho serine; pThr, phospho threonine; Par, parvulin; RMSF, root-mean-square fluctuation

■ REFERENCES

(1) Pace, C. N., Grimsley, G. R., and Scholtz, J. M. (2009) Protein ionizable groups: pK values and their contribution to protein stability and solubility. *J. Biol. Chem. 284*, 13285−13289.

(2) Thurlkill, R. L., Grimsley, G. R., Scholtz, J. M., and Pace, C. N. (2006) pK values of the ionizable groups of proteins. *Protein Sci. 15*, 1214−1218.

(3) Cleland, W. W. (2000) Low-barrier hydrogen bonds and enzymatic catalysis. *Arch. Biochem. Biophys. 382*, 1−5.

(4) Bachovchin, W. W., and Roberts, J. D. (1978) Nitrogen-15 nuclear magnetic resonance spectroscopy. The state of histidine in the catalytic triad of α-lytic protease. Implications for the charge-relay mechanism of peptide-bond cleavage by serine proteases. *J. Am. Chem. Soc. 100*, 8041−8047.

(5) Fisher, Z., Hernandez Prada, J. A., Tu, C., Duda, D., Yoshioka, C., An, H., Govindasamy, L., Silverman, D. N., and McKenna, R. (2005) Structural and kinetic characterization of active-site histidine as a proton shuttle in catalysis by human carbonic anhydrase II. *Biochemistry 44*, 1097−1105.

(6) Cady, S. D., Luo, W., Hu, F., and Hong, M. (2009) Structure and function of the influenza A M2 proton channel. *Biochemistry 48*, 7356−7364.

(7) Wlodawer, A., and Sjölin, L. (1981) Orientation of histidine residues in RNase A: neutron diffraction study. *Proc. Natl. Acad. Sci. U.S.A. 78*, 2853−2855.

(8) Stöckel, J., Safar, J., Wallace, A. C., Cohen, F. E., and Prusiner, S. B. (1998) Prion protein selectively binds copper(II) ions. *Biochemistry 37*, 7185−7193.

(9) Atwood, C. S., Moir, R. D., Huang, X., Scarpa, R. C., Bacarra, N. M. E., Romano, D. M., Hartshorn, M. A., Tanzi, R. E., and Bush, A. I. (1998) Dramatic aggregation of alzheimer Aβ by Cu(II) is induced by conditions representing physiological acidosis. *J. Biol. Chem. 273*, 12817−12826.

(10) Li, S., and Hong, M. (2011) Protonation, tautomerization, and rotameric structure of histidine: a comprehensive study by magic-angle-spinning solid-state NMR. *J. Am. Chem. Soc. 133*, 1534−1544.

(11) Haddad, K. C., Sudmeier, J. L., Bachovchin, D. A., and Bachovchin, W. W. (2005) α-Lytic protease can exist in two separately stable conformations with different His57 mobilities and catalytic activities. *Proc. Natl. Acad. Sci. U.S.A. 102*, 1006−1011.

(12) Ash, E. L., Sudmeier, J. L., Day, R. M., Vincent, M., Torchilin, E. V., Haddad, K. C., Bradshaw, E. M., Sanford, D. G., and Bachovchin, W. W. (2000) Unusual ^{1}H NMR chemical shifts support (His) Cε1—H···O═══C H-bond: proposal for reaction-driven ring flip mechanism in serine protease catalysis. *Proc. Natl. Acad. Sci. U.S.A. 97*, 10371−10376.

(13) Kim, M., Nichols, S., Wang, Y., and McCammon, J. A. (2013) Effects of histidine protonation and rotameric states on virtual screening of *M. tuberculosis* RmlC. *J. Comput.-Aided Mol. Des. 27*, 235−246.

(14) Harris, T. K., and Turner, G. J. (2002) Structural basis of perturbed pKa values of catalytic groups in enzyme active sites. *IUBMB Life 53*, 85−98.

(15) Goedele, R., Nicolas, F., and Joris, M. (2013) Understanding the pKa of redox cysteines: the key role of hydrogen bonding. *Antioxid. Redox Sign. 18*, 94−127.

(16) Zhiyou, Cai, and Yan, L.-J. (2013) Protein Oxidative modifications: beneficial roles in disease and health. *J. Biochem. Pharmacol. Res. 1*, 15−26.

(17) Lang, K., Schmid, F. X., and Fischer, G. (1987) Catalysis of protein folding by prolyl isomerase. *Nature 329*, 268−270.

(18) Yaffe, M. B., Schutkowski, M., Shen, M., Zhou, X. Z., Stukenberg, P. T., Rahfeld, J.-U., Xu, J., Kuang, J., Kirschner, M. W., Fischer, G., Cantley, L. C., and Lu, K. P. (1997) Sequence-specific and phosphorylation-dependent proline isomerization: a potential mitotic regulatory mechanism. *Science 278*, 1957−1960.

(19) Bayer, E., Goettsch, S., Mueller, J. W., Griewel, B., Guiberman, E., Mayr, L. M., and Bayer, P. (2003) Structural analysis of the mitotic regulator hPin1 in solution: insights into domain architecture and substrate binding. *J. Biol. Chem. 278*, 26183−26193.

(20) Schutkowski, M., Bernhardt, A., Zhou, X. Z., Shen, M., Reimer, U., Rahfeld, J.-U., Lu, K. P., and Fischer, G. (1998) Role of phosphorylation in determining the backbone dynamics of the serine/threonine-proline motif and Pin1 substrate recognition. *Biochemistry 37*, 5566−5575.

(21) Ranganathan, R., Lu, K. P., Hunter, T., and Noel, J. P. (1997) Structural and functional analysis of the mitotic rotamase Pin1 suggests substrate recognition is phosphorylation dependent. *Cell 89*, 875−886.

(22) Lu, K. P., and Zhou, X. Z. (2007) The prolyl isomerase PIN1: a pivotal new twist in phosphorylation signalling and disease. *Nat. Rev. Mol. Cell Biol. 8*, 904−916.

(23) Theuerkorn, M., Fischer, G., and Schiene-Fischer, C. (2011) Prolyl cis/trans isomerase signalling pathways in cancer. *Curr. Opin. Pharmacol. 11*, 281−287.

(24) Bulbarelli, A., Lonati, E., Cazzaniga, E., Gregori, M., and Masserini, M. (2009) Pin1 affects Tau phosphorylation in response to Aβ oligomers. *Mol. Cell. Neurosci. 42*, 75−80.

(25) Lu, P.-J., Wulf, G., Zhou, X. Z., Davies, P., and Lu, K. P. (1999) The prolyl isomerase Pin1 restores the function of Alzheimer-associated phosphorylated tau protein. *Nature 399*, 784−788.

(26) Pastorino, L., Sun, A., Lu, P.-J., Zhou, X. Z., Balastik, M., Finn, G., Wulf, G., Lim, J., Li, S.-H., Li, X., Xia, W., Nicholson, L. K., and Lu, K. P. (2006) The prolyl isomerase Pin1 regulates amyloid precursor protein processing and amyloid-[beta] production. *Nature 440*, 528−534.

(27) Zhang, Y., Daum, S., Wildemann, D., Zhou, X. Z., Verdecia, M. A., Bowman, M. E., Lücke, C., Hunter, T., Lu, K.-P., Fischer, G., and Noel, J. P. (2007) Structural basis for high-affinity peptide inhibition of human Pin1. *ACS Chem. Biol. 2*, 320−328.
(28) Greenwood, A., Rogals, M., De, S., Lu, K., Kovrigin, E., and Nicholson, L. (2011) Complete determination of the Pin1 catalytic domain thermodynamic cycle by NMR lineshape analysis. *J. Biol. NMR 51*, 21−34.
(29) Velazquez, H. A., and Hamelberg, D. (2011) Conformational selection in the recognition of phosphorylated substrates by the catalytic domain of human Pin1. *Biochemistry 50*, 9605−9615.
(30) Velazquez, H. A., and Hamelberg, D. (2013) Conformation-directed catalysis and coupled enzyme−substrate dynamics in Pin1 phosphorylation-dependent *cis*−*trans* isomerase. *J. Phys. Chem. B 117*, 11509−11517.
(31) Vöhringer-Martinez, E., Duarte, F., and Toro-Labbé, A. (2012) How does Pin1 catalyze the *cis*−*trans* prolyl peptide bond isomerization? A QM/MM and mean reaction force study. *J. Phys. Chem. B 116*, 12972−12979.
(32) Bailey, M. L., Shilton, B. H., Brandl, C. J., and Litchfield, D. W. (2008) The dual histidine motif in the active site of Pin1 has a structural rather than catalytic role. *Biochemistry 47*, 11481−11489.
(33) Mercedes-Camacho, A. Y., Mullins, A. B., Mason, M. D., Xu, G. G., Mahoney, B. J., Wang, X., Peng, J. W., and Etzkorn, F. A. (2013) Kinetic isotope effects support the twisted amide mechanism of Pin1 peptidyl-prolyl isomerase. *Biochemistry 52*, 7707−7713.
(34) Behrsin, C. D., Bailey, M. L., Bateman, K. S., Hamilton, K. S., Wahl, L. M., Brandl, C. J., Shilton, B. H., and Litchfield, D. W. (2007) Functionally important residues in the peptidyl-prolyl isomerase Pin1 revealed by unigenic evolution. *J. Mol. Biol. 365*, 1143−1162.
(35) Hennig, L., Christner, C., Kipping, M., Schelbert, B., Rücknagel, K. P., Grabley, S., Küllertz, G., and Fischer, G. (1998) Selective inactivation of parvulin-like peptidyl-prolyl *cis/trans* isomerases by juglone. *Biochemistry 37*, 5953−5960.
(36) Aluise, C. D., Rose, K., Boiani, M., Reyzer, M. L., Manna, J. D., Tallman, K., Porter, N. A., and Marnett, L. J. (2012) Peptidyl-prolyl *cis/trans*-isomerase A1 (Pin1) is a target for modification by lipid electrophiles. *Chem. Res. Toxicol. 26*, 270−279.
(37) Sultana, R., Boyd-Kimball, D., Poon, H. F., Cai, J., Pierce, W. M., Klein, J. B., Markesbery, W. R., Zhou, X. Z., Lu, K. P., and Butterfield, D. A. (2006) Oxidative modification and down-regulation of Pin1 in Alzheimer's disease hippocampus: a redox proteomics analysis. *Neurobiol. Aging 27*, 918−925.
(38) Mueller, J. W., Link, N. M., Matena, A., Hoppstock, L., Rüppel, A., Bayer, P., and Blankenfeldt, W. (2011) Crystallographic proof for an extended hydrogen-bonding network in small prolyl isomerases. *J. Am. Chem. Soc. 133*, 20096−20099.
(39) Li, H., Robertson, A. D., and Jensen, J. H. (2005) Very fast empirical prediction and rationalization of protein pKa values. *Proteins: Struct., Funct., Bioinf. 61*, 704−721.
(40) Olsson, M. H. M., Søndergaard, C. R., Rostkowski, M., and Jensen, J. H. (2011) PROPKA3: consistent treatment of internal and surface residues in empirical pKa predictions. *J. Chem. Theory Comput. 7*, 525−537.
(41) Bas, D. C., Rogers, D. M., and Jensen, J. H. (2008) Very fast prediction and rationalization of pKa values for protein−ligand complexes. *Proteins: Struct., Funct., Bioinfo. 73*, 765−783.
(42) Søndergaard, C. R., Olsson, M. H. M., Rostkowski, M., and Jensen, J. H. (2011) Improved treatment of ligands and coupling effects in empirical calculation and rationalization of pKa values. *J. Chem. Theory Comput. 7*, 2284−2295.
(43) Anandakrishnan, R., Aguilar, B., and Onufriev, A. V. (2012) H++ 3.0: automating pK prediction and the preparation of biomolecular structures for atomistic molecular modeling and simulations. *Nucleic Acids Res. 40*, W537−W541.
(44) Myers, J., Grothaus, G., Narayanan, S., and Onufriev, A. (2006) A simple clustering algorithm can be accurate enough for use in calculations of pKs in macromolecules. *Proteins: Struct., Funct., Bioinf. 63*, 928−938.
(45) Gordon, J. C., Myers, J. B., Folta, T., Shoja, V., Heath, L. S., and Onufriev, A. (2005) H++: a server for estimating pKas and adding missing hydrogens to macromolecules. *Nucleic Acids Res. 33*, W368−W371.
(46) Word, J. M., Lovell, S. C., Richardson, J. S., and Richardson, D. C. (1999) Asparagine and glutamine: using hydrogen atom contacts in the choice of side-chain amide orientation. *J. Mol. Biol. 285*, 1735−1747.
(47) Daum, S., Fanghänel, J., Wildemann, D., and Schiene-Fischer, C. (2006) Thermodynamics of phosphopeptide binding to the human peptidyl prolyl *cis/trans* isomerase Pin1. *Biochemistry 45*, 12125−12135.
(48) Guex, N., and Peitsch, M. C. (1997) SWISS-MODEL and the Swiss-Pdb viewer: An environment for comparative protein modeling. *Electrophoresis 18*, 2714−2723.
(49) Warshel, A., Sussman, F., and King, G. (1986) Free energy of charges in solvated proteins: microscopic calculations using a reversible charging process. *Biochemistry 25*, 8368−8372.
(50) Simonson, T., Carlsson, J., and Case, D. A. (2004) Proton binding to proteins: pKa calculations with explicit and implicit solvent models. *J. Am. Chem. Soc. 126*, 4167−4180.
(51) Case, D. A., Cheatham, T. E., Darden, T., Gohlke, H., Luo, R., Merz, K. M., Onufriev, A., Simmerling, C., Wang, B., and Woods, R. J. (2005) The Amber biomolecular simulation programs. *J. Comput. Chem. 26*, 1668−1688.
(52) Hornak, V., Abel, R., Okur, A., Strockbine, B., Roitberg, A., and Simmerling, C. (2006) Comparison of multiple Amber force fields and development of improved protein backbone parameters. *Proteins: Struct., Funct., Bioinf. 65*, 712−725.
(53) Homeyer, N., Horn, A. C., Lanig, H., and Sticht, H. (2006) AMBER force-field parameters for phosphorylated amino acids in different protonation states: phosphoserine, phosphothreonine, phosphotyrosine, and phosphohistidine. *J. Mol. Model. 12*, 281−289.
(54) Jorgensen, W. L. (1982) Revised TIPS for simulations of liquid water and aqueous solutions. *J. Chem. Phys. 77*, 4156−4163.
(55) Ryckaert, J.-P., Ciccotti, G., and Berendsen, H. J. C. (1977) Numerical integration of the cartesian equations of motion of a system with constraints: molecular dynamics of n-alkanes. *J. Comput. Chem. 23*, 327−341.
(56) Izaguirre, J. A., Catarello, D. P., Wozniak, J. M., and Skeel, R. D. (2001) Langevin stabilization of molecular dynamics. *J. Chem. Phys. 114*, 2090−2098.
(57) Essmann, U., Perera, L., Berkowitz, M. L., Darden, T., Lee, H., and Pedersen, L. G. (1995) A smooth particle mesh Ewald method. *J. Chem. Phys. 103*, 8577−8593.
(58) Humphrey, W., Dalke, A., and Schulten, K. (1996) VMD: visual molecular dynamics. *J. Mol. Graphics 14*, 33−38.
(59) DeLano, W. L. (2002) *The PyMOL Molecular Graphics System*, 1.1r1 ed., DeLano Scientific, San Carlos, CA.
(60) Chinea, G., Padron, G., Hooft, R. W. W., Sander, C., and Vriend, G. (1995) The use of position-specific rotamers in model building by homology. *Proteins: Struct., Funct., Bioinf. 23*, 415−421.
(61) Hooft, R. W. W., Sander, C., and Vriend, G. (1996) Positioning hydrogen atoms by optimizing hydrogen-bond networks in protein structures. *Proteins: Struct., Funct., Bioinf. 26*, 363−376.
(62) Barman, A., and Prabhakar, R. (2012) Protonation states of the catalytic dyad of β-secretase (BACE1) in the presence of chemically diverse inhibitors: a molecular docking study. *J. Chem. Inf. Model. 52*, 1275−1287.
(63) Gorfe, A. A., Ferrara, P., Caflisch, A., Marti, D. N., Bosshard, H. R., and Jelesarov, I. (2002) Calculation of protein ionization equilibria with conformational sampling: pKa of a model leucine zipper, GCN4 and barnase. *Proteins: Struct., Funct., Bioinf. 46*, 41−60.
(64) Wang, P.-F., McLeish, M. J., Kneen, M. M., Lee, G., and Kenyon, G. L. (2001) An unusually low pKa for Cys282 in the active site of human muscle creatine kinase. *Biochemistry 40*, 11698−11705.
(65) Kollman, P. A., Massova, I., Reyes, C., Kuhn, B., Huo, S., Chong, L., Lee, M., Lee, T., Duan, Y., Wang, W., Donini, O., Cieplak, P., Srinivasan, J., Case, D. A., and Cheatham, T. E. (2000) Calculating

structures and free energies of complex molecules: combining molecular mechanics and continuum models. *Acc. Chem. Res. 33*, 889−897.
(66) Wang, X. J., Xu, B., Mullins, A. B., Neiler, F. K., and Etzkorn, F. A. (2004) Conformationally locked isostere of phosphoSer−cis-Pro inhibits Pin1 23-fold better than phosphoSer−trans-Pro isostere. *J. Am. Chem. Soc. 126*, 15533−15542.
(67) Namanja, A. T., Wang, X. J., Xu, B., Mercedes-Camacho, A. Y., Wilson, K. A., Etzkorn, F. A., and Peng, J. W. (2011) Stereospecific gating of functional motions in Pin1. *Proc. Natl. Acad. Sci. U.S.A. 108*, 12289−12294.